

# Self-energy limited ion transport in sub-nanometer channels

Douwe Jan Bonthuis<sup>1</sup>, Jingshan Zhang<sup>2</sup>, Breton Hornblower<sup>1,3</sup>,

Jérôme Mathé<sup>1</sup>, Boris I. Shklovskii<sup>2</sup>, and Amit Meller<sup>1\*</sup>

<sup>1</sup> Rowland Institute at Harvard, Harvard University, Cambridge, Massachusetts 02142

<sup>2</sup> William I. Fine Theoretical Physics Institute, University of Minnesota, Minneapolis, Minnesota

<sup>3</sup> Department of Chemistry and Biochemistry, University of California at Santa Cruz, Santa Cruz, California 95060

The current-voltage characteristics of the  $\alpha$ -Hemolysin protein pore during the passage of single-stranded DNA under varying ionic strength,  $C$ , are studied experimentally. We observe strong blockage of the current, weak super-linear growth of the current as a function of voltage, and a minimum of the current as a function of  $C$ . These observations are interpreted as the result of the ion electrostatic self-energy barrier originating from the large difference in the dielectric constants of water and the lipid bilayer. The dependence of DNA capture rate on  $C$  also agrees with our model.

PACS numbers: 87.14.Gg, 87.15.Tt

The voltage-driven translocations of polynucleotides through nanoscale pores has been recently studied *in vitro* at the single molecule level [1, 2]. The dynamics of biopolymer translocation through nanopores is central to many biological processes such as RNA export and phage infection, and is the underlying principal behind a number of new methods for nucleic acids analysis. Single molecule DNA and RNA translocation experiments, as well as theoretical models and simulations have provided some critical information on the dynamics of biopolymer transport and its dependence on physical parameters such as the electric field intensity, polymer length, temperature, and chemical characteristics, such as its sequence [1, 2, 3]. However, much less is known about the nature of the *ion current* during the translocation of the biopolymer through the nanopore.

We use a single  $\alpha$ -Hemolysin ( $\alpha$ -HL) pore embedded in an insulating phospholipid membrane. An ion current of  $I \sim 80$  pA is reduced down to  $I_B \sim 7$  pA upon the electrophoretic threading of single stranded DNA molecule into the pore (Fig. 1), with the ratio  $I_B/I = 0.09$  [4]. Under these conditions the translocation time of a single base in the polynucleotide is  $\sim 5 \mu\text{s}$  [2]. To establish a current of  $\sim 7$  pA approximately 220 ions must flow through the pore in the opposite direction during the passage of a nucleotide. As a first approximation we can therefore assume that the DNA is nearly static compared with the fast moving ions.

Why is  $I_B/I$  so small? The first possible explanation is that the passage of the ssDNA strongly reduces the cross section of the channel available for ionic movement. In a bulk solution ssDNA has the tendency of base stacking leading to formation of a helix with a diameter of  $\sim 1$  nm [5], which is considerably smaller than the averaged channel diameter 1.7 nm [6]). Therefore, such a dramatic current blockage is unlikely to be explained *solely* by the reduced cross section.

In this paper we study how the blocked current  $I_B$  depends on ionic strength  $C$  and voltage  $V$ . We also find that the capture rate of DNA in the pore strongly depends on  $C$ . We explain these observations as a conse-

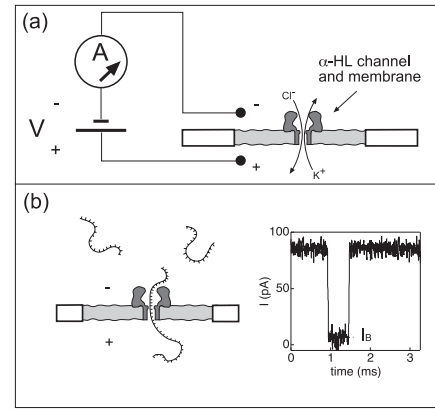


FIG. 1: I-V measurements (a) for an “open” pore, and (b) when single stranded DNA is electrophoretically threaded through the pore. DNA abruptly blocks the ion current from 80 pA to  $\sim 7$  pA ( $I_B$ ), as shown in the inset ( $C = 1$  M KCl,  $V = 120$  mV,  $T = 8^\circ\text{C}$ ).

quence of an electrostatic self-energy barrier [7] related to the huge difference between dielectric constant  $\kappa_1 = 80$  of water and that of lipids and DNA  $\kappa_2 \sim 2$ . This difference results in the confinement of the electric field lines of an ion during the ssDNA passage through the channel, leads to a large self-energy of the ion, and *electrostatically amplifies* the effect of the channel narrowing.

An electrostatic self-energy barrier was predicted by Parsegian [7], but its effects have not been directly observed in the conduction of biological channels. Apparently, evolution has used several compensating mechanisms to facilitate ionic transport (screening by salt, “doping” channels walls by fixed charges and coating of walls by hanging dipoles) [8, 9, 10, 11]. On the other hand, electrostatic barrier was observed in conduction of synthetic ion channels [12], which do not experience evolutionary pressure. Similarly,  $\alpha$ -HL is not known to function as a DNA transporter *in vivo*. Thus, one might expect to observe effects of the self-energy barrier.

Current-voltage ( $I - V$ ) measurements of a unitary  $\alpha$ -

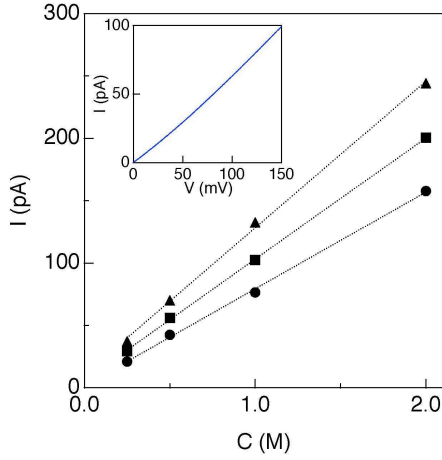


FIG. 2: Open pore current characteristics at  $T = 8^\circ\text{C}$ . The main figure displays the dependence of the current on the bulk KCl concentration measured at  $120\text{mV}$ ,  $150\text{mV}$  and  $180\text{mV}$  (circles, squares and triangles respectively). Lines are linear regression fits. The inset is the measured I-V at  $1\text{ M KCl}$ .

HL were performed using dynamic voltage control [13, 14]. Fig. 2 displays the current for the open pore as a function of  $C$  measured at  $120\text{ mV}$ ,  $150\text{ mV}$  and  $180\text{ mV}$ . In all cases the current follows a linear dependence on  $C$  (thin lines), in the measured range ( $0.25\text{ M} - 2\text{ M}$ ). The inset displays the I-V characteristic curve measured at  $C = 1\text{ M KCl}$ .

The blocked ion current,  $I_B$  (Fig. 3), displays several marked differences as compared to the open pore current. In contrast to the linear dependence of the open pore current on  $C$ , the blocked current is not monotonic. It grows with  $C$  roughly linearly for  $C \geq 1\text{ M}$ , while at  $C < 1\text{ M}$  it changes only weakly and goes through shallow minimum near  $C = 0.5\text{ M}$ . Furthermore, the  $I - V$  curve of  $I_B$  measured at  $1\text{ M KCl}$  (inset of Fig. 3) is more non-ohmic than that of the open pore current displayed in the inset of Fig. 2.

The dependence of the DNA capture rate on the salt concentration is displayed in Fig. 4. Previous studies showed that the capture rate scales linearly with the bulk DNA concentration under similar conditions [15]. The capture rate dependence on  $C$  is highly non-linear: below  $0.5\text{ M KCl}$  the capture rate sharply decreases, and for  $C > 0.5\text{ M}$  it levels off. This trend is consistent for the three different voltages that we measured. Measurements below  $0.25\text{ M}$  were impractical due to the long delay time between events.

We use a crude model to qualitatively interpret the experimental results. Our model is lacking sophistication and quantitative approach of modern theories of ion channels [9, 10], but emphasizes two-dimensional specifics (see below) of DNA translocation physics, which has not been discussed in the literature.

Let us treat ssDNA and the channel internal wall as coaxial cylinders (Fig. 5) with radius  $r = 0.5\text{ nm}$  and  $a =$

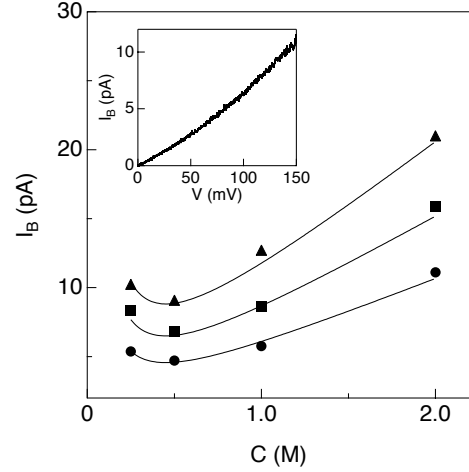


FIG. 3: Main figure: The dependence of the blocked ion current,  $I_B$  on bulk ion concentration measured at  $120\text{mV}$ ,  $150\text{mV}$  and  $180\text{mV}$  (circles, squares and triangles respectively).  $I_B$  values were determined from the peak of the distributions of  $> 1000$  DNA translocation events for each  $C$  and  $V$ . Solid lines are guides to eyes. The inset displays the measured I-V curve for the blocked pore, performed using dynamic voltage control [13, 14].

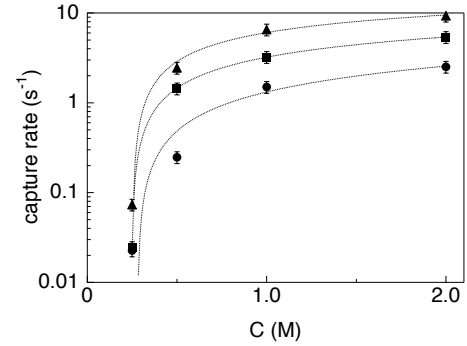


FIG. 4: The dependence of DNA capture rate (per mole) on KCl concentration,  $C$ . Circles, squares and triangles correspond to  $V = 120\text{mV}$ ,  $150\text{mV}$  and  $180\text{mV}$ , respectively

$0.85\text{ nm}$ , respectively. Salt ions are located in the water-filled space between them, with thickness  $d = 0.35\text{ nm}$ . The length of the channel is  $L = 5\text{ nm}$ . Each charge on a ssDNA phosphate in the channel is typically neutralized by a  $\text{K}^+$  ion, forming a pair. In the confined space of the ssDNA-occupied pore,  $\text{K}^+$  ion is strongly bound to a phosphate moiety on the ssDNA backbone. The strong attraction arises from confinement of an electrical field between two cylinders. Within this space opposite charges interact with strong two-dimensional logarithmic potential  $(2e^2/\kappa_1) \ln(\rho/d)$  (see Fig. 6), where  $\rho > d$  is the two-dimensional distance between them. The fact that  $d \simeq l_B/2$ , where  $l_B = e^2/\kappa_1 k_B T = 0.7\text{ nm}$  is the Bjerrum length and  $T$  is the temperature of the experiment, means that  $T \simeq T_c/2$ , where  $T_c = e^2/(k_B \kappa_1 d)$  is the Kosterlitz-Thouless transition temperature [16]. Thus, the thermal

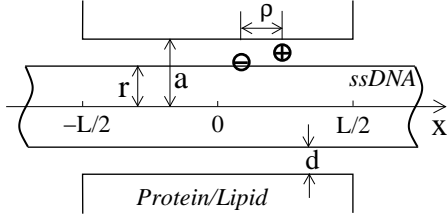


FIG. 5: The side view of the membrane and the channel with DNA inserted. A phosphate and a  $K^+$  ion bound to it are shown.

motion can not break a pair [17].

Considering charge transport we may first ignore neutral pairs. An electric current is produced by an extra ion crossing the channel in the confined space. Such ion has a higher self-energy than ions in the bulk solution, or in other words it goes through an electrostatic self-energy barrier  $U(x)$ . This blocks the ion current. To estimate  $U(x)$  we write  $U(x) = e\phi(x)/2$ , where  $\phi(x)$  is the electrostatic potential created by a charge  $e$  located at  $x$ . Our numerical calculation in the limit of infinite ratio  $\kappa_1/\kappa_2$ , when all electric lines stay in the channel and at  $a/d \gg 1$  can be well fitted by the following expression:

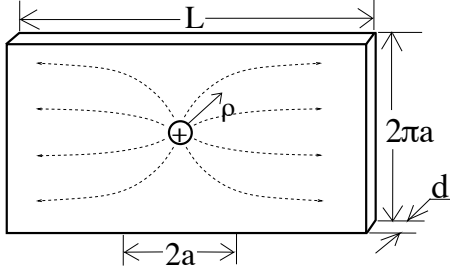


FIG. 6: An unfolded view of the water-filled space containing an extra  $K^+$  ion. Dashed lines represent the electric field lines of the charge. At  $\rho < a$  this electric field spreads in all directions and becomes uniform far from the charge.

$$U(x) = U_1(x) + U_2(x) = \frac{e^2}{\kappa_1 d} \left[ \frac{L}{4a} \left( 1 - \frac{4x^2}{L^2} \right) + \ln \frac{a}{d} \right]. \quad (1)$$

The origin of the two terms in Eq. (1) is illustrated in Fig. 6 for  $x = 0$ . At  $d < \rho < a$  the electric field of the central charge gradually spreads over all azimuthal angles in the whole water-filled space decaying as  $E = e/(\kappa_1 \rho d)$ . This leads to  $\phi(x) = (2e/\kappa_1 d) \ln(a/d)$  and the barrier term  $U_2(x)$ . The  $U_2(x)$  is essentially independent of  $x$  at the distances larger than  $a$  from the ends and but vanishes at the channel ends, where most of electric lines are attracted to the bulk solution (this decay is not reflected by Eq. (1)). On the other hand,  $U_1(0)$  is created by the one-dimensional uniform electric field at distances  $\rho > a$ . For  $|x| > 0$  the electric field at the closer

end is stronger than that of the other end, therefore  $U_1(x)$  decreases parabolically with  $|x|$  and vanishes at the channel ends [11]. For  $L = 5$  nm,  $a = 0.85$  nm and  $d = 0.35$  nm Eq. (1) gives  $U(0) \simeq 4.6 k_B T$ , or  $U_1(0) = 2.9 k_B T$  and  $U_2(0) = 1.7 k_B T$ . The total barrier  $U(x)$  of an extra  $K^+$  or  $Cl^-$  ion is shown on Fig. 7a by the upper curves.

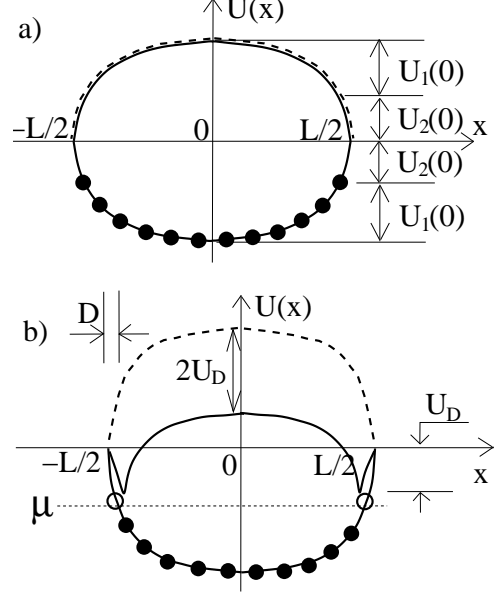


FIG. 7: Energy band diagram for  $K^+$  ions (solid lines) and  $Cl^-$  ions (dashed lines). The lower band represents the energy of the cations bound to DNA phosphates. The empty upper bands show the self-energy of the extra salt cation (solid line) and anions (dashed line) entering the channel. a) In the absence of the Donnan layers ( $C \geq C_D$ ) b) with Donnan layers of the width  $D$  creating potential  $-U_D$ . Vacant phosphates are shown by empty circles. The chemical potential  $\mu$  of  $K^+$  ions in the system is shown by the thin dotted line.

Recall that there are  $K^+$  ions bound to ssDNA phosphates in the channel. Each of them can be removed to the bulk creating a vacancy. The energy penalty for this process is the same as the penalty for placing an extra ion in the same place. Thus, energies of bound  $K^+$  ions are  $-U_1(x) - U_2(x)$  and can be shown by the lower solid curve of Fig. 7a. Vacancies have to overcome the barrier  $U(0)$  to cross the channel.

The large self-energy of extra charges deep in the channel results in accurate neutralization of DNA by salt cations. Such nearly perfect neutralization was observed in molecular dynamics modelling [18] of the channel.

At small salt concentration  $C < C_D$ , some cations close to the channel ends can escape to the bulk because the cations enjoy larger entropy in the solution. As a result there are negative charges in the layer of width  $D$  at each end, and positive screening charge in the adjacent layers of the bulk solution. These double layers of the width  $D$  (see Fig. 7b) produce the Donnan potential  $-U_D$  in the

channel, and prevent remaining cations from leaving the channel. The Donnan potential moves down energies of both cation bands, while bending these bands up in the very ends (Fig. 7b). On the other hand, the energy band of an anions is moved up. This leads to the exclusion of anions from the channel noticed in Ref. [18].

These ideas can be used to interpret the  $I_B(C)$  curves in Fig. 3. At large enough salt concentration of the bulk solution  $C > C_D$ , where  $C_D \sim 1$  M, ion current through the channel should be due to extra salt cations and anions. Therefore the blocked current is proportional to salt concentration  $I_B \propto C$ . On the other hand, at  $C < C_D$  the Donnan potential repels anions and the charge transport is due to cations only. In the first approximation the current  $I_B$  is independent of  $C$ , because Donnan potential  $U_D$  grows with decreasing  $C$ , resulting in a smaller barrier  $U(0)$  and for cations to compensate for the decreasing  $C$ . In the second approximation, at  $C < C_D$  the Donnan potential  $U_D$  changes slightly slower than the chemical potential  $\mu = k_B T \ln(C/C_D)$ . As a result when  $C$  decreases the barrier for vacancies decreases slightly and the barrier for extra cations slightly increases. This leads to vacancy dominated transport [19] and explains the weak increase of  $I_B(C)$  as  $C$  decreases shown in Fig. 3. In the limit of small  $C$  beyond the measured range, we would expect the blocked current to recover  $I_B \propto C$ , as the Donnan potential exceeds the original barrier  $U(0)$ .

Let us switch to the current-voltage characteristics

shown in the inset of Fig. 3. It is super-linear, because the transport is limited by electrostatic barriers shown on Fig. 7. On the other hand, this barrier is relatively flat and therefore the super-linearity should be weak. This agrees with inset of Fig. 3.

Finally let us concentrate on the sharp dependence of DNA capture rate on  $C$  (Fig. 4). It was suggested [20] that DNA loses conformational entropy during translocation, and therefore the DNA capture rate acquires a barrier. However, this mechanism cannot explain the observed  $C$  dependence, because the ssDNA persistence length decreases with  $C$ , making the conformation barrier larger. We notice that the screening cloud of the piece of DNA in the channel is squeezed and corresponding loss of entropy represents a barrier for the DNA capture. This barrier decreases with  $C$  qualitatively explaining the growing capture rate with  $C$ .

To summarize, we studied the dependence of the blocked ion current during DNA translocation on ion concentration. Our experimental results show non-monotonic behavior, which cannot be accounted for by steric blockade alone. We show that these results may be explained by the inclusion of the electrostatic energy of ions inside the pore.

We are grateful to A. Kamenev for useful discussions. We acknowledge support from National Science Foundation grants no. NIRT-0403891 and PHY-0417067.

\* Electronic mail: meller@rowland.harvard.edu

- 
- [1] J. J. Kasianowicz, E. Brandin, D. Branton and D. W. Deamer, Proc. Natl. Acad. Sci. **93**, 13770 (1996); M. Akeson, D. Branton, J. J. Kasianowicz, E. Brandin and D. W. Deamer, Biophys. J., **77**, 3227 (1999); A. Meller, L. Nivon, E. Brandin., J. Golovchenko and D. Branton, Proc. Natl. Acad. Sci. **97**, 1079 (2000).
  - [2] A. Meller, L. Nivon, D. Branton, Phys. Rev. Lett. **86**, 3435 (2001).
  - [3] A. Meller, J. Phys. Cond. Matt. **15**, R581 (2003).
  - [4] This value corresponds to ss-DNA entering the pore with its 3' end, which is the most probable direction [13].
  - [5] W. Saenger, Principles of Nucleic Acid Structure, Springer Verlag New York, (1984)
  - [6] L. Song, M.R. Hobaugh, C. Shustak, S. Cheley, H. Bayley, J.E. Gouaux, Science, **274**, 1859 (1996).
  - [7] A. Parsegian, Nature **221**, 844 (1969); P. C. Jordan, Biophys J. **39**, 157 (1982).
  - [8] D. A. Doyle et al., Science. **280**, 69 (1998); R. MacKinnon, Nobel Lecture. Angew Chem Int Ed Engl **43** 4265 (2004).
  - [9] S. Kuyucak, O. S. Andersen, and S-H. Chung, Rep. Prog. Phys. **64**, 1427 (2001); B. Nadler, U. Hollerbach, R. S. Eisenberg, Phys. Rev. E **68**, 021905 (2003); B. Roux, T. Allen, S. Berneche, W. Im, Quart. Rev. Biophys. **37**, 15 (2004).
  - [10] G. R. Dieckmann, J. D. Lear, Q. Zhong, M. L. Klein, W. F. DeGrado, K. A. Sharp, Biophys. J. **76** 618 (1999); A. B. Mamonov, R. D. Coalson, A. Nitzan, M. Kurnikova, Biophys. J. **84** 3646 (2003); Z. Schuss, B. Nadler, R. S. Eisenberg, Phys. Rev. E, **64** 036116 (2003); A. Burykin, A. Warshel, Biophys. J. **85** 3696 (2003); P. Graf, M. Kurnikova, R. D. Coalson, A. Nitzan, J. Phys. Chem. **108** 2006 (2004)
  - [11] A. Kamenev, J. Zhang, A. I. Larkin, B. I. Shklovskii, Physica A **359**, 129 (2006); J. Zhang, A. Kamenev, B. I. Shklovskii, Phys. Rev. Lett. **95**, 148101 (2005).
  - [12] J. D. Lear, J. P. Schneider, P. K. Kienker, W. F. DeGrado, J. Am. Chem. Soc. **119**, 3212 (1997).
  - [13] J. Mathé, A. Aksimentiev, D. Nelson, K. Schulten and A. Meller, Proc. Natl. Acad. Sci., **102**, 12377 (2005).
  - [14] M. Bates, M. Burns, A. Meller, Biophys. J., **84**, 2366 (2003).
  - [15] S. E. Henrickson, M. Misakian, B. Robertson J. J. Kasianowicz, Phys. Rev. Lett. **85** 3057 (2000); A. Meller D. Branton Electrophoresis **23**, 2583 (2002).
  - [16] J.M. Kosterlitz, D.J. Thouless, J. of Phys. C: Sol. St. Phys., **6** 1181 (1973).
  - [17] One may wonder what happens if the whole DNA cylinder is shifted to one side. It is easy to show that because of spiral location of charges this will leave cations localized.
  - [18] Y. Rabin, M. Tanaka, Phys. Rev. Lett. **94**, 148103 (2005).
  - [19] M. F. Schumaker, R. MacKinnon, Biophys. J. **58**, 975 (1990).
  - [20] T. Ambjörnsson, S. P. Apell, Z. Konkoli, E. A. Di Marzio, and J. J. Kasianowicz, J. Chem. Phys. **117**, 4063 (2002); W. Sung and P. J. Park, Phys. Rev. Lett. **77**, 783 (1996); M. Muthukumar, J. Chem. Phys. **111** 10371, (1999).